THE GLOBAL SPATIAL RANDOMNESS OF IMPACT CRATERS ON MERCURY, VENUS, AND THE MOON. C. Riedel[1,2], G. Michael[2], C. Orgel[3], C. Baum[4], C. H. van der Bogert[5], and H. Hiesinger[5], [1]University of Potsdam, Department of Computer Science, An der Bahn 2, 14476 Potsdam, Germany (christian.riedel@uni-potsdam.de), [2]Freie Universität Berlin, Inst. of Geological Sciences, Malteserstr. 74-100, 12249 Berlin, Germany, [3]European Space Agency, Directorate of Human and Robotic Exploration, Noordwijk, The Netherlands, [4]Aarhus University, Department of Computer Science, Åbogade 34, 8200 Aarhus N, Denmark, [5]Institut für Planetologie, Westfälische Wilhelms-Universität, Wilhelm-Klemm-Str. 10, 48149 Münster, Germany.

Introduction: Impact cratering on a planetary body occurs primarily at spatially random locations. Therefore, a significant non-random distribution of impact craters can indicate the presence of geologic processes that modified the primary impactor record. Such modification can include the erasure of pre-existing craters by geologic processes or the addition of non-primary craters by secondary impacts. In order to detect such phenomena, impact craters on planetary surfaces can be assessed for their spatial randomness.

Often the spatial randomness of crater populations is analyzed using Monte Carlo approaches [1,2]. Such approaches compare a given crater population on a planetary surface to a compilation of randomly generated craters to evaluate their spatial arrangement. The techniques typically use a spatial measure to quantify the spatial relationships between craters (e.g., distances or areas between neighboring craters) and a statistical measure that compares the spatial measures of the given and the randomly distributed crater data sets (e.g., percentile or Z-score) to determine whether a given population is distinguishable from a random one.

Spatial Statistics from Geodesic Measurements: The Craterstats software [3] includes two standardized techniques to quantify the spatial arrangement of impact craters, where the spatial measure is determined by the mean of the second-closest neighbor distances (M2CND) and the standard deviation of the craters' adjacent area (SDAA), determined by a Voronoi triangulation. The implemented techniques measure the neighborhood relationships in a two-dimensional Cartesian coordinate system. Therefore, the obtained results are influenced by map distortion effects that can affect the randomness analysis results. Since the distortions' intensity typically intensifies with increasing distance to the projection center, this issue explicitly affects reference areas that are relatively large compared to the size of the planetary body.

In order to consider the influence of the planetary curvature when measuring the spatial relationships between impact craters, we developed geodesic solutions to the M2CND and SDAA statistics that can be implemented in future software tools. A given crater population is divided into size-dependent and overlapping subpopulations of 300 craters to detect size-dependent variations in the spatial arrangement of impact craters while keeping the computational demands reasonable. In our application, we compare each subpopulation to 100000 randomly distributed crater data sets to quantify their spatial arrangement. We applied the improved methods to global crater datasets of Mercury [4,5], Venus [6], and the Moon [7] and connected the results to known surface evolution scenarios. Where applicable, we investigated crater ($D < 300$ km) and basin populations ($D \geq 300$ km) separately. A random distribution of craters is rejected when a subpopulation's Z score is ≤ -2 or ≥ 2.

Geologic Context:

Mercury. Mercury's volcanic activity significantly influenced its surface evolution and observable cratering record. In its early geologic history, effusive volcanism and global resurfacing events formed Mercury's most ancient surfaces on which today's crater record could accumulate [5]. The extended volcanic processes on Mercury's surface led to the formation of two major geologic units: ancient, densely cratered intercrater plains and more sparsely cratered, younger smooth plains that formed during an era of declining volcanic activity [8].

Venus. Compared to other planetary bodies, Venus hosts few craters. The low crater densities result from extended volcanic activity in its recent geologic history. Two scenarios could describe the resurfacing history of Venus: (1) equilibrium resurfacing or (2) global resurfacing [9]. In the equilibrium scenario, volcanic resurfacing occurred at a constant rate throughout the recent geologic history, and visible craters are erased at the same rate they are produced. In the global resurfacing scenario, intense volcanic activity eliminated all craters that predated the current surface units and visible craters accumulated in an epoch of decreasing and spatially limited volcanic activity.

Moon. Intensive bombardment and volcanism have led to two major geologic units: ancient, heavily cratered highlands and young, sparsely cratered maria. The lunar maria result from flood volcanism which formed within topographic lows [10] and are mostly located on the nearside. The asymmetric distribution of mare deposits has been, for example, attributed to increased volcanic activity due to a thinner crust [11].

Results: The study results are summarized in Figure 1, where the relative fraction of binned crater populations (20 km ≤ D < 300 km) on Mercury, Venus, and the Moon that fall into Z-Score categories of |Z| < 2, 2 ≤ |Z| < 5, 5 ≤ |Z| < 10, and |Z| ≥ 10 is presented. Crater sizes in binned populations are determined by D_{mean} and represented by brightness gradations. The results show that the amount of binned crater populations indistinguishable from a random population is highest on Venus and significantly lower on Mercury and the Moon. Figure 1 also illustrates that the SDAA technique reacts more sensitive to non-random crater configurations on planetary surfaces than the M2CND approach.

Mercury. The results show that many crater subpopulations with D < 300 km are distinguishable from a random distribution at a two-sigma confidence level due to different crater densities on Mercury's smooth plains and intercrater plain deposits. In contrast to the cratering record, randomness is not rejected by either technique for Mercury's basin populations.

Venus. Except for one subpopulation investigated by the SDAA method, all populations were indistinguishable from randomly distributed ones. However, we saw that craters in the non-randomly distributed subpopulation are less abundant in areas of recent volcanic activity, such as Aphrodite Terra and the Beta-Atla-Themis region. Therefore, our results are more consistent with a global resurfacing scenario where Venus' crater record accumulated in a time of decreasing volcanic activity, but where non-random crater populations can occur due to local volcanic resurfacing events in its recent geologic history.

Moon. Randomness was rejected for nearly all binned crater populations due to differences in crater densities between lunar highlands and lunar maria. This confirms that many pre-existing craters were erased by mare volcanism. Our results suggest that mare emplacement in the central Procellarum KREEP Terrane erased craters with D > 100 km. Therefore, lunar mare deposits in this region would have to reach thicknesses of several kilometers to bury such craters. Randomness is not rejected for lunar basins.

References: [1] Michael et al. (2012) *Icarus*, 218, 169-177. [2] Kirchoff (2017) *Meteoritics & Planet. Sci.*, 53, 874-890. [3] Michael & Neukum (2010) *EPSL*, 294, 223-229. [4] Fassett et al. (2011) *Geophys. Res. Lett.*, 38, L17201. [5] Orgel et al. (2020) *JGR Planets*, 125, e2019JE006212. [6] Schaber et al. (1995*) LPSC XXVI*, 1227-1228. [7] Robbins (2019) *JGR Planets*, 124, 871-892. [8] Byrne et al. (2016) *Geophys. Res. Lett.*, 43, 7408-7416. [9] Phillips et al. (1992) *JGR*, 97, 15923. [10] Wilhelms (1987) *USGS Professional Paper 1348*. [11] Miljković et al. (2013) *Science*, 342, 724-726.

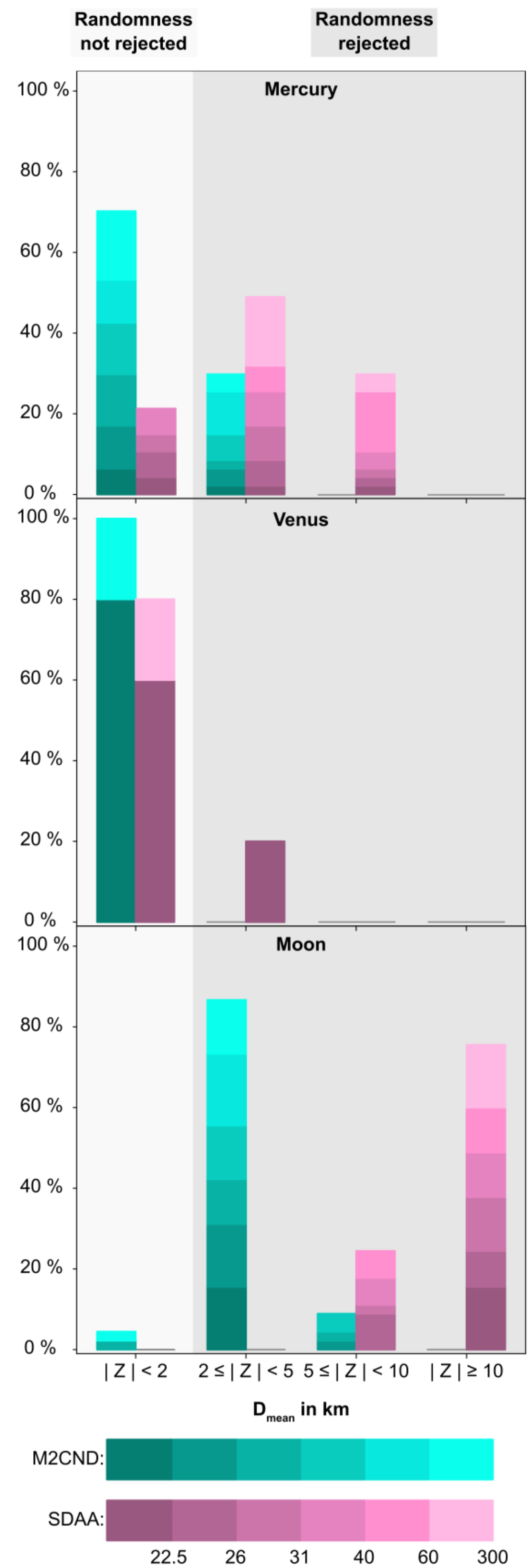

Figure 1: *Z-Scores of binned crater populations from geodesic M2CND and SDAA measurements.*